Paper

Electromagnetic Wave Diffraction by Conducting Flat Strips

Non-member Vladimir V. Veremey (Institute of Radiophysics & Electronics, Ukrainian Academy of Sciences)
Non-member Elder I. Veliev (Institute of Radiophysics & Electronics, Ukrainian Academy of Sciences)
Member Akira Matsushima (Kumamoto University)

An efficient method of solution for problem of wave diffraction by a set of perfectly conducting flat strips is presented, where both E- and H-polarizations are treated. By using a spectral approach, the problem is reduced to a system of linear algebraic equations for the unknown Fourier coefficients of the current density function. A truncation of the infinite system of equations can yield the solution with any desired accuracy. Numerical results are presented for total cross sections of a single strip and strip resonators. By detailed examinations of the convergence in numerical computations, the criteria for truncation size are established. The limitation of this method on the strip width is also revealed.

Keywords: Electromagnetic wave diffraction, Strip scatterers, Integral equations

1. Introduction

It is important to develop an accurate and efficient numerical algorithm for the wave diffraction problems by conducting flat strips, because it is a canonical problems of practical structures such as resonators, reflectors, or polygonal cylinders.

At low frequencies the wave diffraction by a strip is analyzed easily, and this had been the problem in the 1930s when computers were unavailable. For large scatterers compared with the wavelength, simple solutions based on Kirchhoff's method or GTD are applicable. In the resonance region (strip width$\approx 0.5-5.0\lambda$, λ: wavelength), however, we must rely on numerical techniques.

One of the powerful tools is the spectral domain approach that employs Weber-Schafheitlin discontinuous integral, and it has been applied to the strip/slot problems[(1)~(4)]. These are, however, restricted to the case of a single strip/slot. The present authors recently made an analysis of the diffraction by polygonal cylinders[(5)], which includes mutual interactions among different facets, and hence, becomes an extension of Refs (1)~(3) [note that Ref. (4) used different forms of basis functions from the others]. This approach regards each facet as a flat plate, and introduces correct wedge singularities of an induced current, choosing the weighted Gegenbauer polynomials as the bases. Whereas, in the papers above[(1)~(5)], no detailed discussion is given for the relation between the errors and the amount of computational labor.

In the present paper, we will focus our attention only to the configulations constructed by separated strips, which are special cases of Ref. (5). The analysis is then projected on the framework of a set of Chebyshev polynomials. This paper considers both polarizations, although Ref. (5) treated only the case of H-waves. The objectives of this paper are

(i) to extend Refs (1)~(3) to a set of strips, taking the multiple scattering among strip conductors into account,

(ii) to construct the criteria for the truncation size in numerical computations, and

(iii) to reveal the limitation on the strip size.

We use the Fourier transform to the unknown current density, which is expanded in terms of Chebyshev polynomials. Then the problem is reduced to the system of linear algebraic equations for the Fourier coefficients of the current. The solution of the linear equations can be obtained by truncation with any desired accuracy. Numerical results are presented for total cross sections of a single strip and strip resonators.

2. Formulation of the problem

The strips are flat, negligibly thin, and uniform in the z direction. We number them as $p=1,2,\cdots,N$. Fig. 1 shows the cross sections of representative two strips. Let us denote the center of p-th strip by (x_{p0}, y_{p0}) or (r_{p0}, φ_{p0}) in the fixed coordinate system, and also by (r_{pq}, φ_{pq}) in the relative system with regard to q-th strip. We introduce the local coordinates (x_p, y_p) by

$$\begin{pmatrix} x-x_{p0} \\ y-y_{p0} \end{pmatrix}=\begin{pmatrix} \cos\varphi_p & -\sin\varphi_p \\ \sin\varphi_p & \cos\varphi_p \end{pmatrix}\begin{pmatrix} x_p \\ y_p \end{pmatrix} \qquad (1)$$

where the angle φ_p is measured counterclockwise from $\hat{x}$ to $\hat{x}_p$ (the hat denotes a unit vector). The p-th strip lies in $-a_p<x_p<a_p$, $y_p=0$. We assume that the strip conductors do not intersect each other.

Let us derive the integral equations for the surface current density induced on the strips. We divide the total electromagnetic field as

$$E_z^{\text{total}}=E_z^i+E_z \quad \text{(E-wave)} \qquad (2)$$

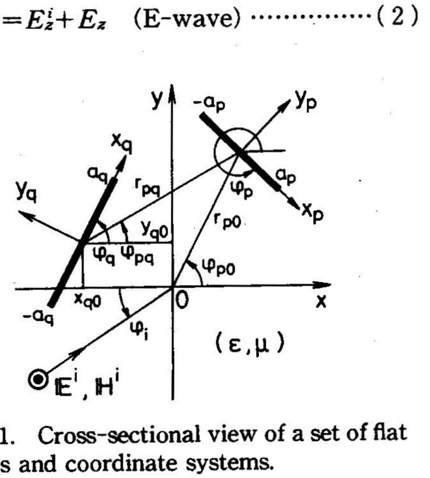

Fig. 1. Cross-sectional view of a set of flat strips and coordinate systems.

$$H_z^{\text{total}}=H_z^i+H_z \quad \text{(H-wave)} \qquad (3)$$

where the superscript i denotes the incident plane wave, and the components without superscript are the scattered fields that are radiated from the current on the strip. With time dependence $e^{-i\omega t}$ assumed, the incident field is written as

$$E_z^i[\zeta H_z^i]=e^{ik(x\alpha_0+y\sqrt{1-\alpha_0^2})} \qquad (4)$$

where $k=\omega\sqrt{\varepsilon\mu}=2\pi/\lambda$, $\zeta=\sqrt{\mu/\varepsilon}$, and $\alpha_0=\cos\varphi_i$ (φ_i: incident angle). Then our objective is to determine E_z and H_z which satisfy

(i) Helmholtz's equation,

(ii) Sommerfeld's radiation condition at infinity,

(iii) Boundary conditions on the strips, and

(iv) Meixner's edge condition.

Employing the conditions (i), (ii) and Green's formulas, we can express the scattered fields as

$$E_z(\boldsymbol{r})=-ik\sum_{q=1}^{N}a_q\int_{-1}^{1}j_z^{(q)}(\eta)G(\boldsymbol{r},\boldsymbol{r}_q(\eta))d\eta \qquad (5)$$

$$\zeta H_z(\boldsymbol{r})=\sum_{q=1}^{N}a_q\int_{-1}^{1}j_x^{(q)}(\eta)\frac{\partial}{\partial y_q}G(\boldsymbol{r},\boldsymbol{r}_q(\eta))d\eta \qquad (6)$$

where $\boldsymbol{r}=x\hat{x}+y\hat{y}$, $\boldsymbol{r}_q(\eta)=x_{q0}\hat{x}+y_{q0}\hat{y}+a_q\eta\hat{x}_q$, $\eta=x_q/a_q$, and the surface current density and Green's function are defined by

$$j_z^{(q)}(\eta)\hat{z}+j_x^{(q)}(\eta)\hat{x}_q=\hat{y}_q\times[\zeta\boldsymbol{H}(\boldsymbol{r}_q(\eta))]_{y_q=-0}^{y_q=+0} \qquad (7)$$

$$G(\boldsymbol{r},\boldsymbol{r}')=(i/4)H_0^{(1)}(k|\boldsymbol{r}-\boldsymbol{r}'|) \qquad (8)$$

[$H_0^{(1)}(x)$: Hankel function]. Using the integral representation of the Hankel function, we have

$$E_z(\boldsymbol{r})=\frac{1}{4\pi}\sum_{q=1}^{N}\int_{-\infty}^{\infty}\bar{j}_z^{(q)}(\alpha) \times e^{ik(x_q\alpha+|y_q|\sqrt{1-\alpha^2})}d\alpha/\sqrt{1-\alpha^2} \qquad (9)$$

$$\zeta H_z(\boldsymbol{r})=-\frac{1}{4\pi}\sum_{q=1}^{N}\text{sgn}(y_q)\int_{-\infty}^{\infty}\bar{j}_x^{(q)}(\alpha) \times e^{ik(x_q\alpha+|y_q|\sqrt{1-\alpha^2})}d\alpha \qquad (10)$$

where the Fourier transform pair has been introduced by ($\kappa_q=ka_q$; $w=z,x$)

$$\left.\begin{aligned} \bar{j}_w^{(q)}(\alpha)&=\kappa_q\int_{-1}^{1}j_w^{(q)}(\eta)e^{-i\kappa_q\alpha\eta}d\eta \\ j_w^{(q)}(\eta)&=\frac{1}{2\pi}\int_{-\infty}^{\infty}\bar{j}_w^{(q)}(\alpha)e^{i\kappa_q\alpha\eta}d\alpha \end{aligned}\right\} \qquad (11)$$

Strictly speaking we must consider the α planes of the same number as the strips, because the Fourier transform axes generally intersect each other. In the present paper, however, we will make formal discussions, assuming the possibility of the linear superposition of the Fourier image of the current by the use of only one variable α as Eqs (9) and (10).

Substituting the expressions of the total field into the boundary conditions (iii) (the Dirichlet and Neumann conditions for E- and H-waves, respectively) and taking the absence of current outside the strips into account, we get the system of dual integral equations ($p=1,2,\cdots,N$)

$$\left.\begin{aligned}&\int_{-\infty}^{\infty}\bar{j}_z^{(p)}(\alpha)e^{i\kappa_p\alpha\eta}\frac{d\alpha}{\sqrt{1-\alpha^2}}\\&\quad=-4\pi e^{iA_p(\eta)}-\sum_{\substack{q=1\\q\neq p}}^{N}\int_{-\infty}^{\infty}\bar{j}_z^{(q)}(\alpha)e^{iB_{pq}(\alpha,\eta)}\\&\qquad\times\frac{d\alpha}{\sqrt{1-\alpha^2}}\qquad(|\eta|<1)\\&\int_{-\infty}^{\infty}\bar{j}_z^{(p)}(\alpha)e^{i\kappa_p\alpha\eta}d\alpha=0\qquad(|\eta|>1)\end{aligned}\right\}\cdots\cdots(12)$$

$$\left.\begin{aligned}&\int_{-\infty}^{\infty}\bar{j}_x^{(p)}(\alpha)\sqrt{1-\alpha^2}e^{i\kappa_p\alpha\eta}d\alpha\\&\quad=-4\pi e^{iA_p(\eta)}\sin(\varphi_p-\varphi_i)\\&\qquad-\sum_{\substack{q=1\\q\neq p}}^{N}\int_{-\infty}^{\infty}\bar{j}_x^{(q)}(\alpha)S_{pq}(\alpha,\varphi_p)e^{iB_{pq}(\alpha,\eta)}d\alpha\\&\qquad\qquad(|\eta|<1)\\&\int_{-\infty}^{\infty}\bar{j}_x^{(p)}(\alpha)e^{i\kappa_p\alpha\eta}d\alpha=0\qquad(|\eta|>1)\end{aligned}\right\}\cdots\cdots(13)$$

where

$$A_p(\eta)=kr_{p0}\cos(\varphi_{p0}-\varphi_i)+\kappa_p\eta\cos(\varphi_p-\varphi_i)\cdots\cdots(14)$$

$$B_{pq}(\alpha,\eta)=kr_{pq}C_{pq}(\alpha,\varphi_{pq})+\kappa_p\eta C_{pq}(\alpha,\varphi_p)\cdots\cdots(15)$$

$$C_{pq}(\alpha,\varphi)=\cos(\varphi-\varphi_q)\alpha+s_{pq}\sin(\varphi-\varphi_q)\times\sqrt{1-\alpha^2}\cdots\cdots(16)$$

$$S_{pq}(\alpha,\varphi)=-s_{pq}\sin(\varphi-\varphi_q)\alpha+\cos(\varphi-\varphi_q)\times\sqrt{1-\alpha^2}\cdots\cdots(17)$$

with the notation $s_{pq}=\text{sgn}[\sin(\varphi_{pq}-\varphi_q)]$. The relation $s_{pq}=1(-1)$ means that the p-th strip lies in the upper (lower) half side of the x_qy_q plane. For convenience of notations, we have assumed that the p-th strip does not cross the x_q axes ($q\neq p$). It is possible to remove this limitation (T-shaped geometry for example), but in this case the expressions of Eqs (14)~(17) become much complicated. Note that the second term in the right hand side of Eqs (12) and (13) for $|\eta|<1$ describes the mutual interactions among strips.

3. Solution of integral equations

Taking Meixner's edge condition (iv) into account, we expand the unknown functions as

$$j_z^{(q)}(\eta)=\sum_{m=0}^{\infty}j_{zm}^{(q)}T_m(\eta)\Big/\sqrt{1-\eta^2}\cdots\cdots(18)$$

$$j_x^{(q)}(\eta)=\sum_{m=1}^{\infty}j_{xm}^{(q)}U_{m-1}(\eta)\sqrt{1-\eta^2}\cdots\cdots(19)$$

where the bases are Chebyshev polynomials

$$\left.\begin{aligned}&T_m(\cos\theta)=\cos(m\theta)\\&U_m(\cos\theta)=\sin[(m+1)\theta]/\sin\theta\end{aligned}\right\}\cdots\cdots(20)$$

Fourier transforms of Eqs (18) and (19) are

$$\bar{j}_z^{(q)}(\alpha)=\kappa_q\pi\sum_{m=0}^{\infty}(-i)^m j_{zm}^{(q)}J_m(\kappa_q\alpha)\cdots\cdots(21)$$

$$\bar{j}_x^{(q)}(\alpha)=\frac{\pi}{\alpha}\sum_{m=1}^{\infty}(-i)^{m-1}mj_{xm}^{(q)}J_m(\kappa_q\alpha)\cdots(22)$$

where $J_n(x)$ is a Bassel function.

We substitute Eqs (21) and (22) into Eqs (12) and (13) for $|\eta|<1$, and employ the Chebyshev polynomials as weighting functions. Thus we have the system of linear algebraic equations

$$\sum_{q=1}^{N}\sum_{n=0}^{\infty}(-i)^nP_{mn}^{E(pq)}j_{zn}^{(q)}=Q_m^{E(p)}$$
$$(p=1,2,\cdots,N;\ m=0,1,\cdots)\cdots\cdots(23)$$

$$\sum_{q=1}^{N}\sum_{n=1}^{\infty}(-i)^{n-1}nP_{mn}^{H(pq)}j_{xn}^{(q)}=Q_m^{H(p)}$$
$$(p=1,2,\cdots,N;\ m=1,2,\cdots)\cdots\cdots(24)$$

where

$$P_{mn}^{E(pq)}=\kappa_q(2\kappa_p)^{-1}\int_{-\infty}^{\infty}e^{ikr_{pq}C_{pq}(\alpha,\varphi_{pq})}\times J_m(\kappa_pC_{pq}(\alpha,\varphi_p))J_n(\kappa_q\alpha)\frac{d\alpha}{\sqrt{1-\alpha^2}}\cdots\cdots(25)$$

$$P_{mn}^{H(pq)}=\frac{1}{2}\int_{-\infty}^{\infty}e^{ikr_{pq}C_{pq}(\alpha,\varphi_{pq})}\frac{S_{pq}(\alpha,\varphi_p)}{C_{pq}(\alpha,\varphi_p)\alpha}\times J_m(\kappa_pC_{pq}(\alpha,\varphi_p))J_n(\kappa_q\alpha)d\alpha\cdots\cdots(26)$$

$$Q_m^{u(p)}=-2R^{u(p)}e^{ikr_{p0}\cos(\varphi_{p0}-\varphi_i)}\times J_m(\kappa_p\cos(\varphi_p-\varphi_i))\cdots\cdots(27)$$

with $R^{E(p)}=\kappa_p^{-1}$ and $R^{H(p)}=\tan(\varphi_p-\varphi_i)$.

Employing the property of Weber-Schafheitlin discontinuous integral, we can confirm that Eqs (12) and (13) for $|\eta|>1$ are automatically satisfied. Note that the present solution becomes identical to those of Refs (1)~(3) if we set $N=1$ in Eqs (5)~(27).

4. Evaluation of integrals

The evaluation methods of the integrals in Eqs (25) and (26) are summarized below.

4.1 Analytical treatment when $p=q$

The parity of the integrand leads us to

$$P_{mn}^{E(pp)}=\int_0^{\infty}J_m(x_p\alpha)J_n(x_p\alpha)\frac{d\alpha}{\sqrt{1-\alpha^2}}\cdots\cdots(28)$$

$$P_{mn}^{H(pp)}=\int_0^{\infty}J_m(x_p\alpha)J_n(x_p\alpha)\frac{\sqrt{1-\alpha^2}}{\alpha^2}d\alpha\cdots\cdots(29)$$

if $m+n$ is even, and they are zero if $m+n$ is odd. We divide the contour into two parts $(0,1)$ and $(1,\infty)$, and apply the formulas given in Refs (6) and (1) to the respective parts. Then we have

$$\mathrm{Re}P_{mn}^{u(pp)}=\frac{x_p^{m+n}}{3-\xi^u}\sum_{l=0}^{\infty}\tilde{\Gamma}_{mnl}^{u}x_p^{2l}\cdots\cdots(30)$$

$$\mathrm{Im}P_{mn}^{u(pp)}=\frac{1}{(3-\xi^u)\pi}\left[-\sum_{l=0}^{(m+n)/2-1}\Gamma_{mnl}^{u}x_p^{2l}+x_p^{m+n}\sum_{l=0}^{\infty}\tilde{\Gamma}_{mnl}^{u}\psi_{mnl}^{u(p)}x_p^{2l}\right]\cdots\cdots(31)$$

where $\xi^E=1$, $\xi^H=-1$ and

$$\Gamma_{mnl}^{u}=\Gamma\left(l+\frac{\xi^u}{2}\right)\Gamma\left(l+\frac{1}{2}\right)\Gamma\left(\frac{m+n}{2}-l\right)\Big/\left[\Gamma\left(\frac{m+n}{2}+l+1\right)\Gamma\left(\frac{m-n}{2}+l+1\right)\times\Gamma\left(\frac{n-m}{2}+l+1\right)\right]\cdots\cdots(32)$$

$$\tilde{\Gamma}_{mnl}^{u}=(-1)^l\Gamma\left(\frac{m+n}{2}+l+\frac{\xi^u}{2}\right)\times\Gamma\left(\frac{m+n}{2}+l+\frac{1}{2}\right)\Big/[\Gamma(l+1)\Gamma(m+l+1)\Gamma(n+l+1)\times\Gamma(m+n+l+1)]\cdots\cdots(33)$$

$$\psi_{mnl}^{u(p)}=2\log x_p+\psi\left(\frac{m+n}{2}+l+\frac{\xi^u}{2}\right)+\psi\left(\frac{m+n}{2}+l+\frac{1}{2}\right)-\psi(l+1)-\psi(m+l+1)-\psi(n+l+1)-\psi(m+n+l+1)\cdots\cdots(34)$$

with a gamma function $\Gamma(x)$ and a digamma function $\psi(x)=\Gamma'(x)/\Gamma(x)$.

4.2 Numerical treatment when $p\neq q$

Because we cannot generally reduce Eqs (25) and (26) to closed forms, numerical evaluations are required. We first introduce the changes of variables $\alpha=\cos\theta$ and $\alpha=\cosh\theta$ for $|\alpha|<1$ and $|\alpha|>1$, respectively. This cancels the singularities of the integrand at $|\alpha|=1$. Moreover the decrement of the integrand as $|\alpha|\to\infty$ becomes a doubly exponential type. This enables us to employ numerical quadrature formulas, after truncating the infinite contour by a finite one.

5. Far scattered field

Let us introduce the cylindrical coordinate system (r,φ) by the relations $x=r\cos\varphi$ and $y=r\sin\varphi$. Substituting the asymptotic expression of the Hankel function into Eqs (5) and (6), one can write the far field in the form

$$E_z[\zeta H_z]\sim\sqrt{2/(\pi kr)}\,e^{i(kr-\pi/4)}\Phi^{E(H)}(\varphi)\quad(r\to\infty)\cdots\cdots(35)$$

where the pattern functions are written as

$$\Phi^{E}(\varphi)=\frac{\pi}{4}\sum_{q=1}^{N}x_q\sum_{m=0}^{\infty}i^m j_{zm}^{(q)}\tilde{J}_{mq}(\varphi)\cdots\cdots(36)$$

$$\Phi^{H}(\varphi)=-\frac{\pi}{4}\sum_{q=1}^{N}\tan(\varphi-\varphi_q)\sum_{m=1}^{\infty}j^{m-1}m\times j_{xm}^{(q)}\tilde{J}_{mq}(\varphi)\cdots\cdots(37)$$

with $\tilde{J}_{mq}(\varphi)=e^{-ikr_{q0}\cos(\varphi-\varphi_{q0})}J_m(x_q\cos(\varphi-\varphi_q))$. The total scattering cross section is obtained from

$$\sigma_T=2(\pi k)^{-1}\int_0^{2\pi}|\Phi^{E,H}(\varphi)|^2d\varphi\cdots\cdots(38)$$

The error on the optical theorem is defined by

$$\varepsilon_{\rm opt}=2|\sigma_T-\tilde{\sigma}_T|/|\sigma_T+\tilde{\sigma}_T|\cdots\cdots(39)$$

where $\tilde{\sigma}_T=-(4/k)\mathrm{Re}\Phi(\varphi_i)$.

6. Numerical results

6.1 Convergence and accuracy

Let us confirm the convergence and accuracy of the method by examining the total scattering cross section for a single strip ($N=1, r_{10}=\varphi_{10}=0$) at normal incidence ($\varphi_i=\pi/2$). We will construct the criteria for the truncation size, referring Tables 1 and 2. For Eqs (23) and (24) the equations and terms are retained up to $m,n=M$, and for Eqs (30) and (31) up to $l=L$. Unless stated, the computation is done by the use of the double precision (16-digit in Fortran).

Table 1 tells us how to choose the proper number M. As M increases, the cross sections approach the exact values[7] for $ka_1=4$ and 8, and becomes stable up to 5-6 decimal places for $ka_1=12$. For a fixed

Table 1. Convergence of the total scattering cross section for a single strip at normal incidence. Dependence on M.

(a) E-wave

M	$\sigma_T/(4a_1)$		
	$ka_1=4$	$ka_1=8$	$ka_1=12$
2	0.994642	1.004148	1.009558
4	0.998949	0.998871	1.003111
6	0.998956	0.999824	1.000627
8	0.998956	0.999763	1.000647
10	0.998956	0.999756	1.000180
12	0.998956	0.999756	1.000123
14	0.998956	0.999756	1.000121
16	0.998956	0.999756	1.000121
18	0.998956	0.999756	1.000121
exact[7]	0.99896	0.99976	—

(b) H-wave

M	$\sigma_T/(4a_1)$		
	$ka_1=4$	$ka_1=8$	$ka_1=12$
2	0.997822	0.947193	0.935853
4	0.931685	1.023672	1.000852
6	0.942217	0.985744	1.015425
8	0.942435	1.019783	0.990447
10	0.942436	1.023231	1.009241
12	0.942436	1.023318	1.006758
14	0.942436	1.023319	1.004605
16	0.942436	1.023319	1.004399
18	0.942436	1.023319	1.004391
exact[7]	0.94244	1.02332	—

accuracy, wider strips require larger numbers of M. To achieve the convergence up to 5-6 decimal places, it is sufficient to set $M=[ka_1]+4$ ($[x]$: the greatest integer not exceeding x).

Table 2 is employed to determine the number L. We introduce the relative value $\tilde{L}(=L/[ka_1+1])$, because larger L is desired as ka_1 increases. The cross section and the error on the optical theorem become stable when we choose $\tilde{L}=3$ and 4, respectively. From this we can conclude setting $L=4([ka_1+1])$ is sufficient.

Next we discuss the limitation of the method on the strip size in Fig. 2. The notation sng. means that summing in Eqs (30) and (31) was done by the single precision (7-digit). Following the above criteria on M and L, we plotted the error on the optical theorem. The errors are sensitive to the number of digits, because the evaluations of the alternating series in Eqs (30) and (31) are accompanied by subtractive cancellations. If we set

Table 2. Convergence of the total scattering cross section for a single strip at normal incidence. Dependence on $\tilde{L}\,(=L/[ka_1+1])$.

(a) E-wave

$\tilde{L}$	$ka_1=4$		$ka_1=8$	
	$\sigma_T/(4a_1)$	ε_{opt}	$\sigma_T/(4a_1)$	ε_{opt}
2	0.996276	1.3×10^{-3}	0.695261	1.7×10^{-1}
3	0.998956	3.4×10^{-9}	0.999756	8.6×10^{-11}
4	0.998956	3.1×10^{-12}	0.999756	2.8×10^{-10}
5	0.998956	3.1×10^{-12}	0.999756	2.8×10^{-10}
exact[7]	0.99896	—	0.99976	—

(b) H-wave

$\tilde{L}$	$ka_1=4$		$ka_1=8$	
	$\sigma_T/(4a_1)$	ε_{opt}	$\sigma_T/(4a_1)$	ε_{opt}
2	0.942433	1.1×10^{-6}	1.023256	3.1×10^{-5}
3	0.942435	4.3×10^{-12}	1.023318	2.9×10^{-12}
4	0.942435	3.2×10^{-12}	1.023318	2.9×10^{-12}
5	0.942435	3.2×10^{-12}	1.023318	2.9×10^{-12}
exact[7]	0.94244	—	1.02332	—

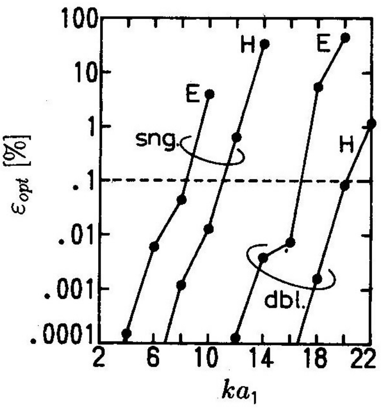

Fig. 2. Comparison of the error on the optical theorem between the single (sng.) and double (dbl.) precision calculations.

the permissible error at 0.1% (3 significant figures), $ka_1\leq16(\leq20)$ must be hold for E- and (H-) waves. These maximum widths are reduced by half in the sng. results.

We further compared with the tables in Ref. (2) ($ka_1\leq5$; normal and oblique incidence) and Ref. (3) ($ka_1\leq16$; normal incidence). Because the analyses are equivalent, agreement must be complete. Whereas, in some data, slight discrepancies (less than 3) were observed at the last figure. As regards Ref. (4), infinite integrals concern the spherical

Bessel functions (due to the different bases), and then require numerical quadratures. The present approach is therefore more advantageous than Ref. (4) from the viewpoint of CPU time. The merit of Ref. (4) is the applicability to wider strips ($ka_1 \leq 10\pi$).

6.2 Strip resonators

Fig. 3 shows the frequency dependence of the total scattering cross section for a parallel strip resonator. The resonances concern the excitations of quasi-natural oscillations: the first peak at $ka_1 \approx 1.2 \approx \pi/2$ (the second peak at $ka_1 \approx 3.3 \approx \pi$) corresponds to the resonance between the open ends (between the strip walls).

Similar characteristics for a square strip resonator are shown in Fig. 4. The resonance property is prominent especially for narrow slots.

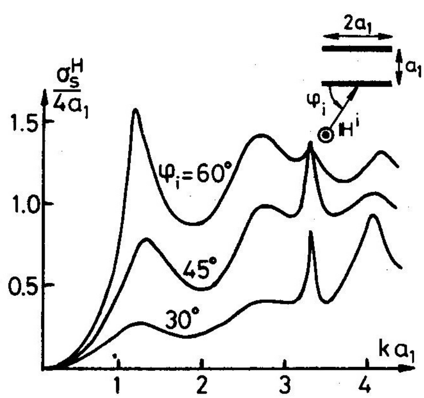

Fig. 3. Frequency dependence of the total scattering cross section for a parallel strip resonator at H-wave incidence.

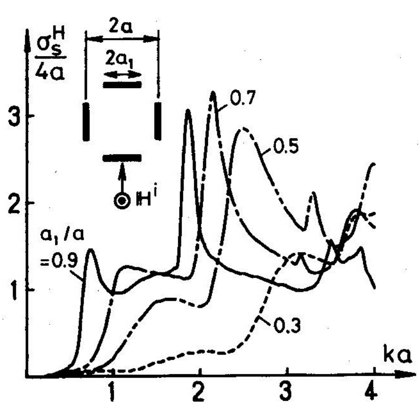

Fig. 4. Frequency dependence of the total scattering cross section for a square strip resonator at H-wave incidence.

Let us discuss the solid line ($a_1/a = 0.9$) for example. The first peak at $ka \approx 0.8 \approx \pi/(2\sqrt{2})$ is due to the renonance between the diagonal slots. Besides, near the second peak at $ka \approx 1.9 \approx \pi/2$, the field formation is close to one of the internal eigenmodes of the closed ($a \times a$) waveguide.

7. Conclusion

We have developed a powerful approach to the wave diffraction problems by a set of perfectly conducting flat strips. By examining the accuracy of the numerical solution for a single strip, the criteria for truncation sizes have been established. We found that the number of significant figures for the far field is more than 3 if the strip is narrower than 5λ (λ: wavelength), which means the method covers the resonance region. We furthermore carried out computations for some strip resonators, and showed their physical properties.

We can extend this method to smoothly curved strips. Nevertheless, we have no proof yet with regard to the possibility of the linear operation of the Fourier images, which was assumed in the spectral representation of the scattered fields. This is the future problem.

(Manuscript received July 22, '92,
revised Dec. 28, '92)

References

(1) Y. Nomura & S. Katsura: "Diffraction of electromagnetic waves by ribbon and slit I", *J. Phys. Soc. Japan*, **12**, 190 (1957)

(2) K. Hongo: "Diffraction of an electromagnetic plane wave by an infinite slit embedded in an anisotropic plasma", *J. Appl. Phys.*, **43**, 4996 (1972)

(3) T. Otsuki: "Reexamination of diffraction problem of a slit by a method of Fourier-orthogonal functions transformation", *J. Phys. Soc. Japan*, **41**, 2046 (1976)

(4) K. Uchida, T. Noda & T. Matsunaga: "Electromagnetic wave scattering by a conducting strip——Spectral domain analysis——", *Trans. IEICE*, **J72-C-I**, 717 (1989) (in Japanese)

(5) E. I. Veliev, V. V. Veremey & V. P. Shestopalov: "Electromagnetic wave diffraction on polygonal cylinders—New approach", Proc. 1989 URSI Int. Symp. on Electromagnetic Theory, Stockholm, p. 628

(6) A. P. Prudnikov, Y. A. Brichkov & O. I. Marichev: Integrals and Series—Special Functions (1983) Nauka, Moscow (in Russian); Japanese Trans.: Sin Sûgaku Kôsiki Syû II—Tokusyu Kansû (1992) Maruzen, Tokyo

(7) S. Skavlem: "On the diffraction of scalar plane waves by a slit of infinite length", *Arch. Math. Naturv.*, **B-51**, 61 (1951)

Vladimir V. Veremey (Non-member)

He was born in Kramatorsk, Ukraine, on Nov. 11, 1956. He graduated from Kharkov State University, and received the Ph. D. degree from the same university in 1984. He is currently a Senior Research Scientist at Institute of Radiophysics and Electronics, Ukrainian Academy of Sciences, Kharkov. His research interests are diffraction theory, numerical-analytical methods in electromagnetic field theory and theory of multireflector antennas and open resonators.

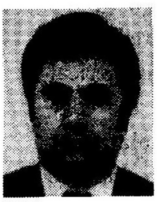

Elder I. Veliev (Non-member)

He was born in Baku, Azerbaijan, on Jan. 24, 1951. He graduated from Azerbaijan State University in 1973. He received the Ph. D. and the Dr. Sci. degrees from Kharkov State University in 1977 and 1988, respectively. He is currently a Leading Research Scientist at Institute of Radiophysics and Electronics, Ukrainian Academy of Sciences, Kharkov. His main interest of research is numerical-analytical methods in electromagnetic boundary value problems.

Akira Matsushima (Member)

He was born in Kumamoto on March 21, 1958. He received the B. E. degree from Kumamoto University in 1980, and the M. E. degree from Kyushu University in 1982. Since 1982, he has been a Research Assistant of Department of Electrical Engineering and Computer Science at Kumamoto University. He is currently working in the area of numerical methods for electromagnetic scattering problems.